MECHANICS OF STRENGTHENING IN CRYSTALLINE ROCK AT LOW TEMPERATURES: A PRELIMINARY ASSESSMENT

Charles G. Sammis and Ronald L. Biegel

University of Southern California

Sponsored by Air Force Research Laboratory

Contract No. DTRA01-01-C-0086

ABSTRACT

Mellor (1973) measured the uniaxial compressive and tensile strengths of granite, limestone, and sandstone over a range of temperatures from 20ºC to –197ºC. For each of the three rock types, he tested both air-dry and water-saturated samples. These data were modeled using the micromechanical damage model. This model was formulated by Ashby and Sammis (1990) by assuming that the primary role of the frozen water in the cracks is to increase the coefficient of friction through the formation of crack-bridging "ice asperities", in addition to the usual rock asperities. The rock asperities are far below their melting temperature and deform by dislocation glide, which is only weakly temperature dependent. The ice asperities, however, form at their melting temperature and therefore deform initially by diffusion-limited creep mechanisms, which are strongly temperature dependent. The strengthening of the ice asperities with falling temperature explains the observed monotonic increase in compressive and tensile strengths at progressively lower temperatures. It also explains the leveling off of strength at very low temperatures where ice is sufficiently below its melting temperature that it deforms by glide, just like the rock asperities. The model is most suitable for low porosity crystalline rock-like granite where Mellor (1973) observed a 35% increase in compressive and a 55% increase in tensile strength between 0 and -120ºC. One important implication of our model is that the effective coefficient of friction, and hence the compressive strength, is both temperature and strain-rate dependent. At the high strain rates in an explosive source, the 35% increase in strength should occur over a much smaller range of temperatures close to 0ºC. The observed strengthening in granite is the same for both the air-dry and saturated samples, whereas, in both limestone and sandstone the saturated samples strengthen much more than do the air-dry samples. This is probably due to the fact that the starter flaws in granite are very thin cracks which are effectively saturated by adhered water films in the air-dry state, while the filling of the more spherical pores in the sandstone and, to a lesser extent, the limestone preferentially increases their mechanical strength in the saturated frozen state. The damage mechanics model is able to qualitatively and quantitatively explain all observed differences between the low temperature behavior of the three rock types and between the dry and saturated states in each. This preliminary assessment of the mechanisms responsible for strengthening rock at low temperature should help guide the design of future low-temperature experiments, and suggests that low-temperature triaxial strength testing should be supplemented with low-temperature friction experiments.

OBJECTIVES

The objectives of this research program are as follows:

1. Build the micromechanical damage mechanics developed by Ashby and Sammis (1990) into source models for underground explosions.
2. Use this model to explore the influence of site effects such as rock type, ground water saturation, permafrost, and depth of burial on the seismic signature generated by the explosion.
3. Use this model to help interpret laboratory measurements and field experiments.
4. Explore the possibility that secondary radiation generated by the damage contributes to the regional seismic phases.

RESEARCH ACCOMPLISHED

Introduction

The Soviet test site at Novaya Zemlya at 73° north latitude lies well above the Arctic Circle. Rock at this site is probably below the freezing point of water to considerable depth. Permafrost thickness is greatest in non-glaciated polar regions like Siberia, where a record depth of 4,900 feet to the permafrost base has been reported. Permafrost thickness in arctic Canada has been estimated to exceed 3,000 feet and in arctic Alaska it may exceed 2,000 feet. The question has therefore arisen as to how frozen water in cracks and pores might affect the seismic signature of an underground explosion.

Uniaxial compressive and tensile tests at a low temperature have shown that freezing can increase rock strength by a factor of four in porous rock and by a factor of 1.8 in crystalline rock (Mellor, 1973). In this paper, we interpret these data using the micromechanical damage model (Ashby and Sammis, 1990) in which sliding on preexisting cracks in rock induces additional fracture damage and ultimate failure. The effect of ice in this model is to increase the effective coefficient of sliding friction on the preexisting cracks thus inhibiting the generation of new damage and strengthening the rock. In addition to strengthening, the damage model is also able to explain some of the more subtle phenomenology in the ice data such as the differences between porous and crystalline rock and the progressive strengthening observed to occur as the temperature is lowered from 0°C to -150°C.

The strengthening associated with low temperatures can be expected to significantly reduce the apparent radius of an explosion by suppressing crack growth in the non-linear damage zone, thus producing a higher frequency seismic signature than that from an equivalent explosion in rock above 0°C. Also, the "pulse broadening" phenomena observed for shots in crystalline rock, which has been associated with dynamical weakening of the damage zone, should be suppressed in frozen crystalline rock. These effects can be assessed quantitatively using the source model developed by Johnson and Sammis (2001), which incorporates the Ashby and Sammis (1990) damage mechanics.

The Uniaxial Strength of Frozen Rock

Mellor (1973) measured the uniaxial compressive and tensile strength of granite, limestone, and sandstone over a temperature range from 20°C to -197°C for both water saturated and air-dry samples. Results from the compressive tests are shown in Figure1 and those from the tensile tests in Figure 2. We first make a few observations about these results and offer a qualitative explanation of each in terms of the damage mechanics model. A more quantitative model for the granite data is given in the next section.

Observation 1: In compression, the saturated samples for all three rock-types show a strong increase in strength beginning at 0°C and continuing to -120°C. The air-dry limestone and sandstone samples do not show a comparable increase in strength at low temperatures. However, both the air-dry and saturated granite samples strengthen at approximately the same rate with decreasing temperature.

Damage Mechanics Explanation: In the saturated samples for all three rock-types, frozen water inhibits sliding on the preexisting flaws, suppressing damage and strengthening the samples. The flow strength of ice increases as the temperature falls below the freezing point thus increasing the apparent coefficient of friction and strengthening the samples. For the air-dry limestone and sandstone specimens, there is not enough adsorbed water in the pores to

provide this strengthening. However, for granite the preexisting microcracks are much narrower. The adsorbed water in the air-dry samples effectively saturates these cracks, and hence there is little difference between the low temperature compressive strength of saturated and air-dry granite. Note that the saturated granite is significantly weaker at $20°$. This may be due to hydrolytic weakening which is suppressed below $0°$C.

Observation 2: In tension, the saturated samples again all show an increase in strength beginning at $0°$C and increasing to lower temperatures. However, in tension, none of the air-dry samples showed a comparable increase in strength. Even the air-dry granite samples remain significantly weaker than the saturated ones at low temperature.

Damage Mechanics Explanation: Failure in tension is nucleated at the largest most dangerously oriented flaw, which grows unstably to produce macroscopic failure. Failure in compression is a cooperative phenomenon involving structures created by the interaction of a myriad of smaller flaws. The reason that the tensile strength in air-dry granite does not track that of the saturated granite, is that the largest crack (the one responsible for the tensile failure) is too large to be saturated by the films of adsorbed water that saturate the myriad of smaller microcracks responsible for compressive failure.

We now quantify these observations by including the effect of frozen water in the Ashby and Sammis (1990) damage mechanics model for granite.

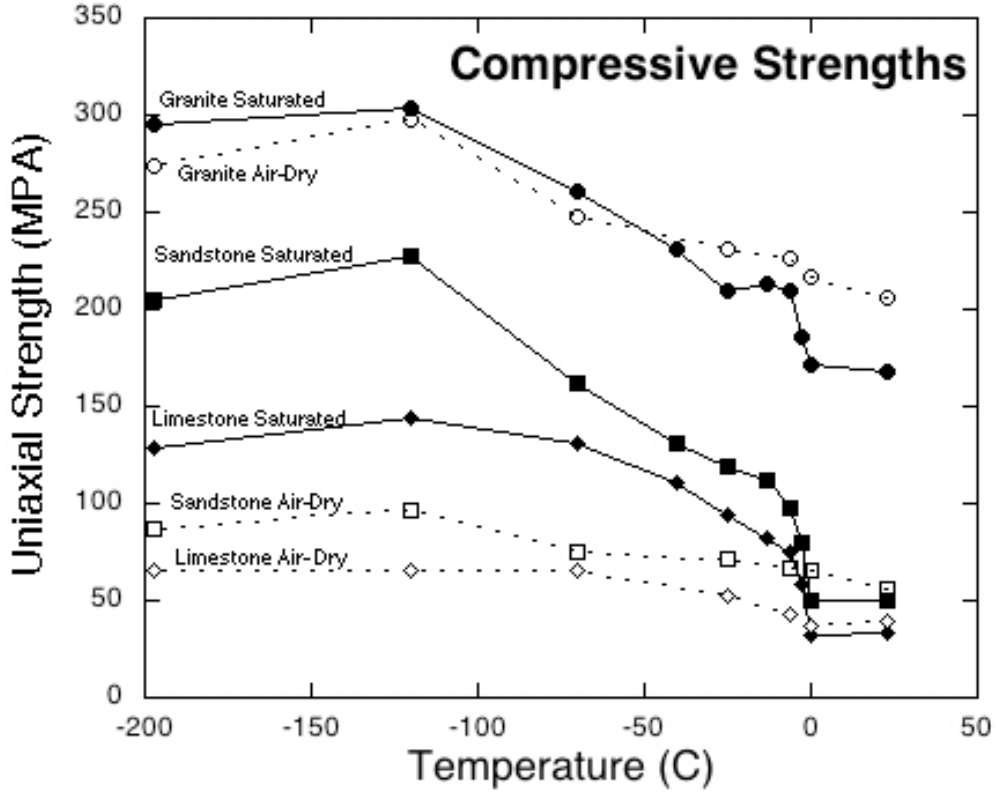

Figure 1. Strength of granite, limestone, and sandstone in uniaxial compression at low temperatures from Mellor (1973). Note that only in granite are the strengths of saturated and air-dry samples nearly the same at all temperatures.

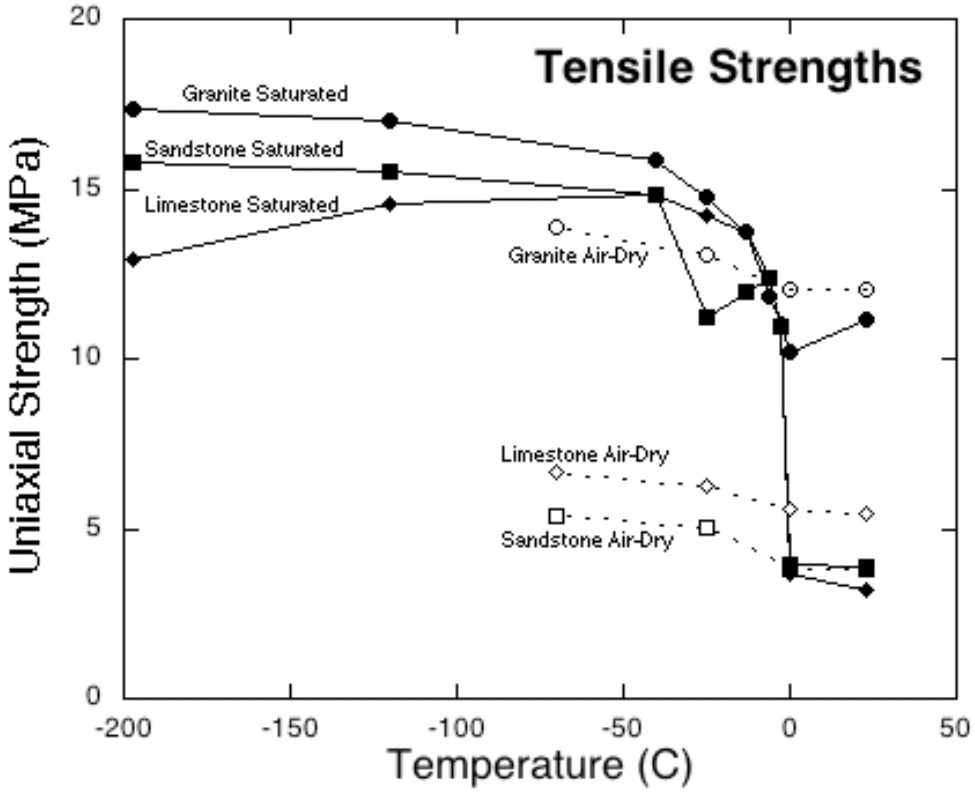

Figure 2. Strength of granite, limestone, and sandstone in uniaxial tension at low temperatures from Mellor (1973). Note that the saturated samples for all three rock-types show more strengthening at low temperatures than do the air-dry samples.

A Damage Mechanics Model for the Strength of Frozen Granite

Ashby and Sammis (1990) show that an initial inclined crack will nucleate tensile wing cracks (as illustrated in Figure 3) when

$$S_1 = C_1 S_3 + S_o \tag{1}$$

where

$$S_1 = \frac{\sigma_1 \sqrt{\pi a}}{K_{Ic}} \qquad C_1 = \frac{\left(1+\mu^2\right)^{1/2} + \mu}{\left(1+\mu^2\right)^{1/2} - \mu}$$

$$S_3 = \frac{\sigma_3 \sqrt{\pi a}}{K_{Ic}} \qquad S_o = \frac{\sqrt{3}}{\left(1+\mu^2\right)^{1/2} - \mu}$$

Using the published value for the critical stress intensity factor $K_{Ic} = 1$ MPa m$^{1/2}$, Ashby and Sammis (1990) fit equation. (1) to data for the initiation of microcrack damage in granite to determine μ in the range 0.55 to 0.65 and a crack length 2*a* near 1 mm. The assumption is that the cracks do not interact during nucleation so that equation. (1) is independent of the initial crack density.

The failure curve is sensitive to the initial crack density, which (in 3D) is expressed by the initial damage defined as

$$D_0 = \tfrac{4}{3}\pi\left(a\cos\chi\right)^3 N_V\,, \tag{2}$$

where χ is angle describing the orientation of the cracks (see Figure. 3) and N_V is the number of cracks per unit volume. In response to loading above the nucleation stress, wing cracks of length l grow at opposite edges of the initial crack thereby increasing the damage to

$$D = \tfrac{4}{3}\pi\left(l + a\cos\chi\right)^3 N_V\,. \tag{3}$$

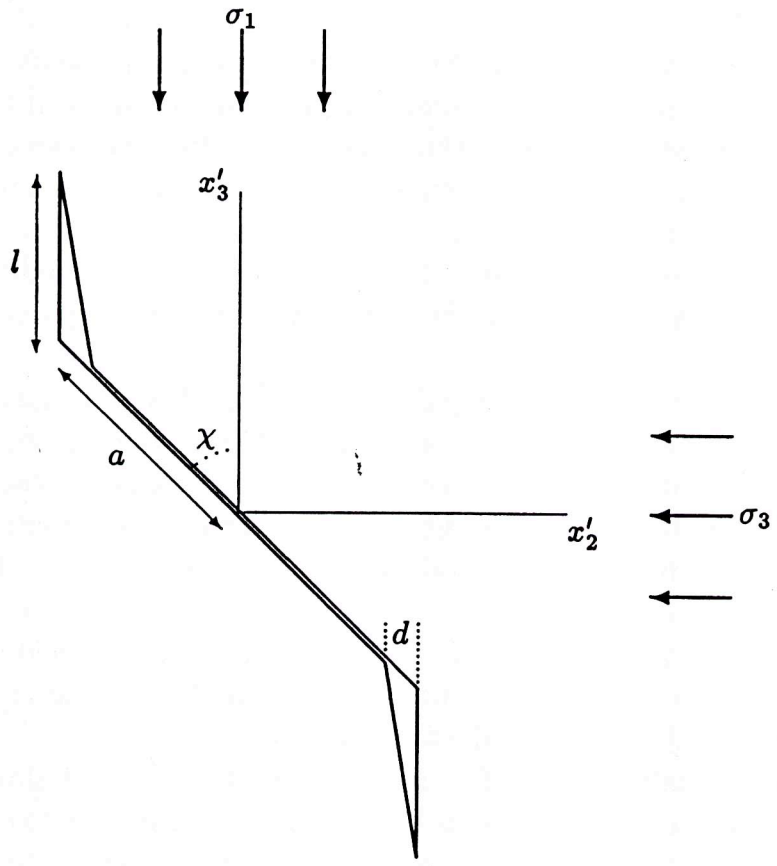

Figure 3. Geometry of a penny-shaped crack of radius *a,* that is extended by wing cracks of length *l*.

The value of l is determined by letting the wing cracks grow until the stress intensity factor at the tip decreases to the fracture toughness of the medium. The equation that relates the equilibrium damage to the initial damage and the dimensionless principal stresses is (Ashby and Sammis, 1990)

$$S_1 = -\frac{C_2\left(\left(\frac{D}{D_0}\right)^{1/3} - 1 + \frac{\beta}{\cos\chi}\right)^{3/2} - S_3\left[C_1\left(1 + \left(\frac{C_3 D_0^{2/3}}{1-D^{2/3}}\right)\left(\left(\frac{D}{D_0}\right)^{1/3} - 1\right)^2\right) + C_4\left(\left(\frac{D}{D_0}\right)^{1/3} - 1\right)^2\right]}{1 + \frac{C_3 D_0^{2/3}}{1-D^{2/3}}\left(\left(\frac{D}{D_0}\right)^{1/3} - 1\right)^2} \tag{4}$$

Where S_1 and S_3 are the maximum and minimum normalized principal compressive stresses defined above. The constants in (4) are

$$\begin{aligned} C_1 &= \frac{\left(1+\mu^2\right)^{1/2} + \mu}{\left(1+\mu^2\right)^{1/2} - \mu} \\ C_2 &= \pi\left(\cos\chi\right)^{3/2}\sqrt{3/\beta}\,\frac{1}{\left(1+\mu^2\right)^{1/2} - \mu} \\ C_3 &= 2 \\ C_4 &= 2\pi\left(\cos\chi\right)^{2}\sqrt{3/\beta}\,\frac{1}{\left(1+\mu^2\right)^{1/2} - \mu} \end{aligned} \tag{5}$$

In equations (5), β is a correction factor for the effective length of the crack, typically 0.45, introduced by Ashby and Sammis (1990) to bring their approximate analytical model into agreement with numerical simulations in the limit of small *l*. Also, crack orientation χ is assumed here to be 45°.

When equation. (4) is used to plot S_1 as a function of *D* (for fixed values of D_o, S_3 and the other parameters), S_1 has a maximum value which Ashby and Sammis (1990) interpret as the failure stress. For larger values of *D* beyond this peak, S_1 decreases. This weakening rheology leads to shear localization and macroscopic failure. Fitting the uniaxial strength of dry granite at $20°\mathrm{C}$ using the values of *a* and μ deduced above from the nucleation gives an initial damage of $D_o = 0.1$.

We now ask how much of an increase in μ is required to produce the compressive strengthening at low temperatures observed in Figure (1). Holding all the other parameters constant, we increased μ to get the uniaxial strength measured by Mellor (Figure1). Figure 4 shows the value of μ as a function of temperature required by this damage mechanics interpretation of Mellors data.

The Apparent Coefficient of Friction of Frozen Cracks

The coefficient of friction μ is defined by Amonton's Law that relates the shear stress τ required to initiate sliding between two surfaces that are supporting a normal stress σ.

$$\tau = \mu\sigma \tag{6}$$

In the case where the boundary contains a fluid with pressure *P*, friction is described by the apparent friction law

$$\tau = \mu(\sigma - P) \tag{7}$$

The coefficient of friction shows the smallest variation of any mechanical parameter across different rock types. Known as "Byerlee's Law", $\mu \approx 0.6$ for virtually all rock surfaces independent of hardness.

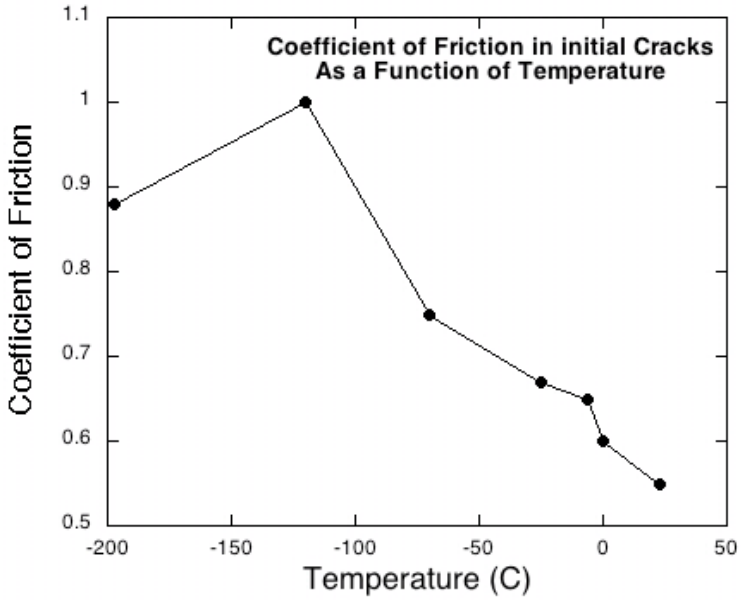

Figure 4. Coefficient of friction on starter cracks required if the damage mechanics model is to explain the increase in compressive strength at low temperatures in Figure 1.

The asperity model for friction, initially formulated by Bowden and Tabor (1950, 1964) offers a simple physical explanation for the constancy of μ. This model recognizes that all surfaces are rough at some scale, and that actual contact occurs at a limited number of high points called asperities. Under a normal load σ the asperities flow thereby increasing the true area of contact, A_c, until the stress on the asperities falls to the normal yield stress, σ_y, of the rock. If the apparent area of the contacting surfaces is *A*, we have

$$\sigma A = \sigma_y A_c \tag{8}$$

The shear stress τ required to initiate sliding is determined by the shear yield stress τ_y at which the asperities fail in shear, which gives:

$$\tau A = \tau_y A_c \tag{9}$$

Equations (8) and (9) may be combined to write

$$\tau = \left(\frac{\tau_y}{\sigma_y}\right)\sigma \tag{10}$$

which is just Amonton's law where $\mu = \tau_y / \sigma_y$. To see why the ratio τ_y / σ_y is nearly independent of rock type, consider the strength of a single asperity with cross-section A_c that is loaded to the compressive yield stress σ_y. This asperity will fail when the maximum shear stress reaches τ_y. As illustrated by the Mohr Circle in Fig 5 the normal yield stress is related to the shear yield stress by $\tau_y / \sigma_y = 0.5$, independent of the material.

If the area between the asperities is saturated with water, this will have no direct effect on μ, as long as $P<<0$. However, if this water freezes, the shear resistance will increase to

$$\tau = \tau_{y_{rock}} \frac{A_{c_{rock}}}{A} + \tau_{y_{ice}} \frac{A_{c_{ice}}}{A} \tag{11}$$

Assuming that the normal load is supported entirely by the rock asperities such that

$$\sigma = \sigma_{y_{rock}} \frac{A_{c_{rock}}}{A} \tag{12}$$

we can express the ice strengthening by an apparent coefficient of friction μ' as

$$\mu' = \frac{\tau}{\sigma} = \frac{\tau_{y_{rock}} A_{c_{rock}} + \tau_{y_{ice}} A_{c_{ice}}}{\sigma_{y_{rock}} A_{c_{rock}}} = \mu + \frac{\tau_{y_{ice}}}{\sigma_{y_{rock}}} \frac{A_{c_{ice}}}{A_{c_{rock}}} \tag{13}$$

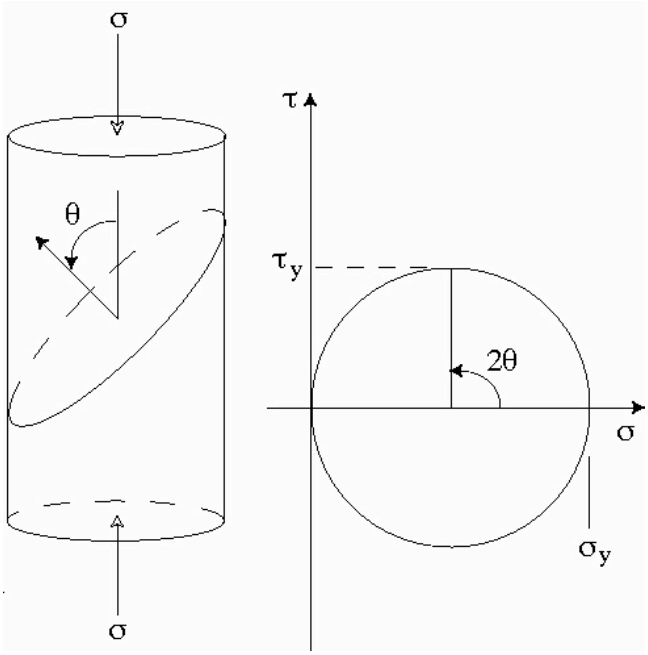

Figure 5. Stress state for a cylindrical asperity loaded to its compressive yield stress σ_y. Note that $\tau_y = 0.5\sigma_y$ where τ_y is the shear strength.

Direct observation of asperities in transparent silicates has shown that they deform by plastic flow (Dieterich and Kilgore, 1996). At the high stresses and low homologous temperature (T/T_m where T_m is the melting temperature) in the rock asperities, the flow stress is nearly independent of strain-rate or temperature. However, the flow stress in ice near its melting temperature is determined by thermally activated diffusion limited creep mechanisms that are very sensitive to both temperature and strain-rate. This is why μ rises rapidly just below $0°\text{C}$ in Figure 1. In equation (13), this behavior is caused by the rapid increase in $\tau_{y_{ice}}$ with falling temperature below $0°\text{C}$. At very low temperatures, flow in the ice will also be controlled by glide and μ' will be almost independent of temperature and strain-rate.

Flow in ice near its melting point is more complicated than high temperature flow in rock. There is a poorly understood change in activation energy at about $-10°\text{C}$ thought to be associated with the suppression of pressure melting at grain boundaries below this temperature (Goodman et al., 1981; Duval et al., 1983). We will take the analysis in this paper one step further by assuming a generic form for this high temperature power-law flow in ice:

$$\dot{\varepsilon} = B\tau^n \exp\left(-Q/RT\right) \tag{14}$$

Solving for the flow stress gives

$$\tau_{y_{ice}} = \left(\frac{\dot{\varepsilon}}{B}\right)^{1/n} \exp\left(Q/nRT\right) \tag{15}$$

Using this in equation. (13) and combining constants gives

$$\mu' = \mu + D\exp\left(Q/nRT\right) \tag{16}$$

or, equivalently,

$$\ln(\mu' - \mu) = \ln D + Q/nRT \tag{17}$$

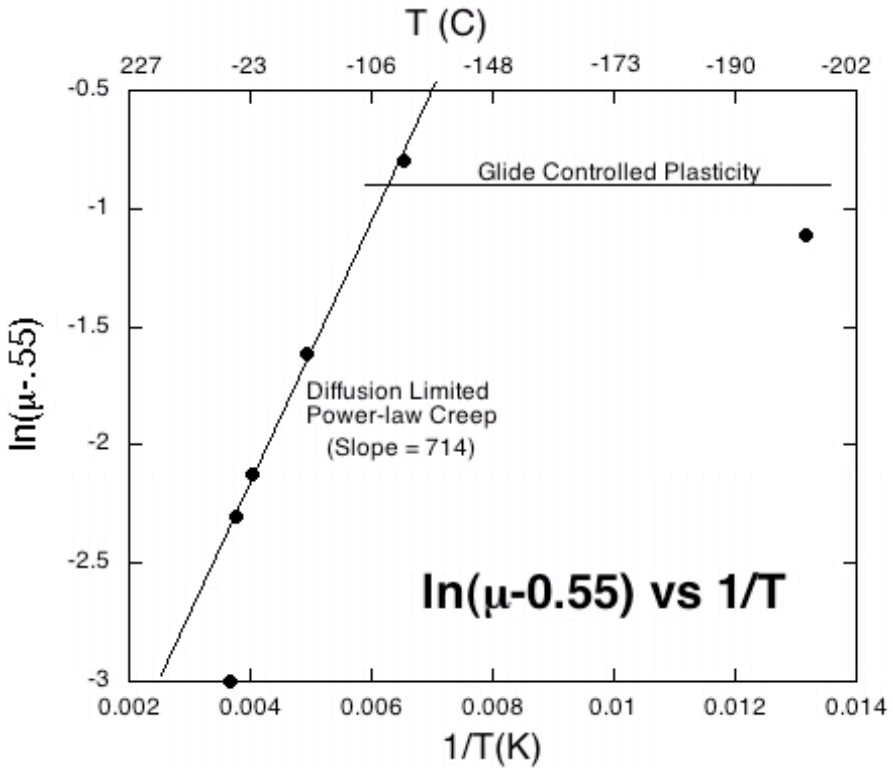

Figure 6. Plot of equation (17) in the text. The slope in the thermally activate region gives $Q/nR = 714$. At temperatures below about 110°C the mechanisms changes to glide controlled plasticity.

In Figure6, $\ln(\mu' - \mu)$ is plotted as a function of 1/T. The linear portion has a slope of $Q/nR = 714$. Below 8.3° C, the activation energy for power law creep is $Q \approx 80$ KJ mole^{-1}(Goodman et al., 1981). This implies a creep power of

$$n = \frac{8x10^4}{(714)(8.3)} = 13.5 \tag{18}$$

This is significantly higher than $n \approx 3$ observed at stresses below 1MPa. However, *n* for ice is observed to rise rapidly at stresses above one MPa (Goodman et al., 1981), so this may simply reflect a higher flow stress on the asperities.

CONCLUSIONS AND RECOMMENDATIONS

The preliminary analysis of rock strength at low temperatures has led to the following conclusions:

1. The basic characteristics of the low temperature uniaxial strength data from Mellor (1973) can be explained by ice in the initial pores and cracks.

2. For uniaxial compression in granite, the observed strengthening at low temperature can be quantitatively modeled using the micromechanical damage model formulated by Ashby and Sammis (1990). In this model the role of the ice is to increase the apparent coefficient of sliding friction on the initial cracks. The temperature dependence of power law creep in the ice asperities near their melting temperature explains the progressive strengthening observed in granite between $0°\mathrm{C}$ and $-150°$.
3. The strengthening at low temperatures should also be strain-rate dependent. At high loading rates, as in an underground explosion, the full strengthening should occur over a limited range of temperatures near $0°\mathrm{C}$.
4. The effect of frozen rock on the seismic signature of an underground explosion can be investigated using source models that include the micromechanical damage model such as that formulated by Johnson and Sammis (2001).

The following recommendations are based on the preliminary analysis in this paper:

1. The uniaxial data from Mellor (1973) should be supplemented with a full set of triaxial data in granite at low temperatures. Uniaxial data typically shows large experimental scatter, mostly because the strength is extremely sensitive to the initial flaw distribution in the absence of confining stress. A set of triaxial data would allow a more comprehensive assessment of the extent to which the damage model can represent the strength of rock at low temperatures.
2. The triaxial data set should be supplemented with measurements of the coefficient of friction as a function of temperature under saturated and air-dry conditions. These measurements can be made either on saw-cut samples as part of the triaxial set of experiments, or in Jim Dieterich's double-shear apparatus at the United States Geological Survey laboratory in Menlo Park, California.
3. Both the triaxial measurements and friction measurements should be performed at different strain-rates to further test the hypothesis that the strengthening is associated with ice asperities.
4. The Johnson and Sammis (2001) model for explosions in granite should be rerun with larger friction coefficients to assess the changes in seismic radiation caused by frozen rock.

REFERENCES

Ashby, M. F., S. and C. G. Sammis (1990), The damage mechanics of brittle solids in compression, *Pure appl. Geophys,* 133, 489-521.

Bowden, F.P., and Tabor D. (1950) *The Friction and Lubrication of Solids. Part I,* Clarenden Press, Oxford.

Bowden, F.P., and Tabor D. (1964) *The Friction and Lubrication of Solids. Part II,* Clarenden Press, Oxford.

Dieterich, J.H., and B.D. Kilgore, Imaging surface contacts: Power law contact distributions and contact stresses in quartz, calcite, glass, and acrylic plastic, *Tectonophysics*, *256*, 219-239, 1996.

Duval, P., M. F. Ashby, and I. Anderman (1983), Rate controlling processes in the creep of polycrystalline ice, *J. Phys. Chem.,* 87, 4066-4074.

Goodman, D. J., H. J. Frost, and M. F. Ashby (1981), The plasticity of polycrystalline ice, *Phil. Mag. A*, 43, 665-695.

Johnson, L. R. and C. G. Sammis (2001), Effects of rock damage on seismic waves generated by explosions, *Pure Appl. Geophys,* 158, 1869-1908.

Mellor, M. (1973), Mechanical properties of rocks at low temperatures, Second International Conference on Permafrost, National Academy of Sciences, Washington, D.C., 334-343.